

# State-of-Health Estimation for Lithium-Ion Batteries in Real-Time Embedded Applications.

Prasant Sethi

College of Engineering Bhubaneswar

**Abstract**— Determining the lithium-ion batteries' state of health (SOH) is essential to making sure they run securely and last a long time. Due to restrictions in the hardware components, the current methods for estimating SOH on embedded systems only take into account one health indicator (HI) to represent either capacity or internal resistance (IR) behavior. However, neither capacity nor IR could be disregarded as they both offer useful battery health information. We thus provide the SOH estimate approach, which can express it using HIs that can be directly monitored in embedded systems with less complex composition, and can take into account both capacity degradation and IR expansion. The suggested approach, according to the data, decreases the inference time by an average of 29.20% and increases estimation accuracy by at least 47.59%. The suggested method's correctness and efficacy are demonstrated and confirmed through the use of many datasets in an actual embedded system.

## I. INTRODUCTION

Nowadays, lithium-ion batteries are frequently employed as the primary power source in a variety of applications, including home appliances, electronics, and electric cars. [1]. It is imperative to properly manage a battery to ensure both safety and longevity. With a battery management system (BMS), this is possible. One of the key functions of a BMS is the state-of-health (SOH) estimation, which provides valuable data to shield the battery from early failure and to increase its durability. [2]. Precise SOH estimations can avert malfunctions that may arise from using a low-charge battery continuously. Numerous strategies have been put out to increase the accuracy of the SOH estimation. Certain researchers have employed model-based techniques, such the equivalent circuit model (ECM) and the electrochemical model. [3]–[5]. Liu *et al.* [3] suggested an ECM based on internal resistance (IR) increase for SOH estimate. The simulated model's excellent accuracy is demonstrated by the result [3], however the accuracy of the battery model affects the model's performance. Eddahecharol. [4] calculated SOH utilizing the data in IR growth

. IR is monitored using impedance spectroscopy. Although the model in [4] has high simulation accuracy, it is difficult to simulate impedance spectroscopy in embedded systems since it requires complex battery data analysis to represent the behavior of IR. To achieve SOH estimation in embedded systems, Verma *et al.* [5] proposed a reduced-order ECM. The model in [5] has been implemented in an embedded system and the performance accuracy increases by 3% compared to the conventional ECM. Nonetheless, the ECM-based model is not able to accurately generalize for other types of batteries. That is, the ECM-based models need to be redeveloped to characterize the behavior of other types of batteries.

To cope with the drawbacks of the above approaches, Chemali [6] used data-driven methods instead of using ECM to perform SOH estimation. The result shows that the model can capture the uncertainties of capacity degradation due to the model's adaptability to nonlinear systems. Although data-driven methods have several advantages, challenges still exist in terms of algorithm design and computation time for embedded system applications. Qu *et al.* [7] utilized a deep learning technique to estimate SOH based on capacity degradation. This process is time consuming and has a high-power demand. Since calculating the battery capacity requires complex integration operations which is not suitable for real-time applications with embedded systems.

Therefore, several researchers have proposed novel health indicators (HIs) as a substitute for battery capacity data to achieve implementation for real-time applications with embedded systems [8], [9]. Shen *et al.* [8] used the voltage, current, and charging capacity to estimate SOH. Despite the use of HIs in [8], the algorithm still requires high memory and power of embedded systems due to complex integration from the capacity calculation. To reduce complexity in extracting HI, Chaoui and Ibe-Ekeocha [9] used measurable battery data, such as voltage, charge/discharge currents, and ambient temperature variations as HIs to substitute capacity degradation. Although these studies used HIs to estimate SOH, the HIs are used to reflect the capacity degradation only which disregards the influence of IR growth. On the other hand, IR growth and capacity degradation are equally important factors for accurate SOH estimation [10]. Particularly, capacity degradation represents battery aging which indicating when a battery should be replaced and IR growth provides the failure indication, thus neither of these could be neglected. Hence, we propose the SOH estimation method that considers both capacity degradation and IR growth by representing it with HIs that can be directly measured in an embedded system with less complex computation.

The contributions of this letter are as follows.

- 1) We utilized HIs that can be extracted without complex computation which enables real-time SOH estimation.

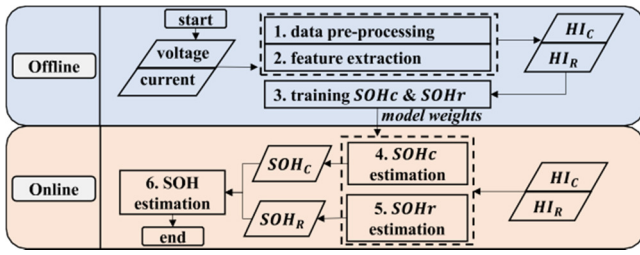


Fig. 1. Flowchart of the proposed SOH estimation.

 TABLE I  
 SPECIFICATION OF BATTERIES DATASETS AND THE CORRELATION COEFFICIENTS BETWEEN HIS AND IR/CAPACITY

Datasets	Initial Capacity (Ah)	Cut-off Voltages (V)	The Correlation Coefficients	
			$HI_R$ reflecting IR growth	$HI_C$ reflecting capacity degradation
BEXEL cell #7	7.08	2.5, 4.2	0.956	0.948
BEXEL cell #13	7.14	2.5, 4.2	0.982	0.943
NASA cell #6	2.04	2.5, 4.2	0.921	0.870
NASA cell #7	1.89	2.2, 4.2	0.948	0.889

- 2) To improve the SOH estimation accuracy, we utilized the relationship between capacity degradation and IR growth.

## II. SOH ESTIMATION MODEL

The proposed SOH estimation is illustrated in Fig. 1. We utilized HIs that are directly measurable using embedded systems applications. The HIs are fed to a recurrent neural network (RNN) that estimates both 1) SOH based on capacity degradation ( $SOH_c$ ); and 2) SOH based on an IR growth ( $SOH_r$ ). To improve the SOH estimation accuracy, the relationship between  $SOH_c$  and  $SOH_r$  was analyzed.

### A. Extraction of Health Indicators

We extracted HIs from two different battery datasets:

1) NASA [11] and 2) BEXEL [12]. Both NASA and BEXEL datasets are extracted from lithium-ion batteries. These datasets consist of the measured voltage, current, temperature, capacity, and IR. Measurements are performed during charging under constant current constant voltage (CC+CV) profile and during constant current discharging. The charge-discharge profile of two battery datasets is listed in Table I. Specifically, the NASA dataset provides information of four cells: 1) cell#5; 2) cell#6; 3) cell#7; and 4) cell#18, whereas the BEXEL dataset provides the same for two cells: a) cell#7; and b) cell#13. These numbers are cell IDs assigned by NASA and BEXEL to identify the cells.

The measured capacity and IR data are required for estimating the SOH, but the NASA dataset only provides IR data of cell#6 and cell#7. Therefore, we only used these cells from the NASA dataset. In the HIs extraction process, we divided the HIs into two categories: 1) HIs that reflect the capacity degradation; and 2) those that reflect the IR growth. To analyze the correlation between these HIs and the corresponding output, we used the Person correlation coefficient which is defined as

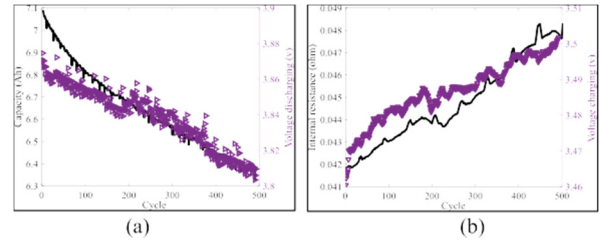


Fig. 2. (a) HIs reflecting the capacity degradation. (b) HIs reflecting an increase in IR.

follows [13]:

$$\rho(A, B) = \frac{1}{N-1} \sum_{i=1}^N \frac{A_i - \mu_A}{\sigma_A} \frac{B_i - \mu_B}{\sigma_B} \quad (1)$$

where  $N$  is the number of observations,  $A$  is HIs,  $B$  is capacity or IR,  $\mu_A$  and  $\mu_B$  are the mean values of  $A$  and  $B$ , and  $\sigma_A$  and  $\sigma_B$  are the standard deviation of  $A$  and  $B$ .

1) *HIs Reflecting Capacity Degradation*: In terms of SOH estimation, capacity degradation is the main factor because it indicates the degradation of battery health. To reduce the computational complexity, capacity degradation is replaced with the first voltage value in the discharging process. The relationship between the charging-discharging cycle with the: 1) first voltage value in the discharging process ( $HI_C$ ); and 2) capacity degradation is shown in Fig. 2(a). As shown in the figure, both the capacity and  $HI_C$  degrade with an increasing number of cycles. In addition to that, the correlation coefficients between  $HI_C$  and capacity degradation are represented in Table I. It shows the correlation coefficients between  $HI_C$  and capacity degradation are greater than 0.8 using the NASA dataset and even greater than 0.9 for the BEXEL dataset. Therefore,  $HI_C$  was found to be capable of reflecting the capacity degradation. Accordingly,  $HI_C$  is used to estimate the SOH based on capacity.

2) *HIs Reflecting Increase in Internal Resistance*: The IR growth in a battery is also used as an indicator of battery health. To reduce the computational complexity, we replaced the IR with the value that corresponds to the first voltage value during the charging process ( $HI_R$ ). The  $HI_R$  and the IR versus cycle are shown in Fig. 2(b). As shown in the figure, both IR and voltage increase with the number of cycles. That is,  $HI_R$  of the first and last cycles is 3.462 and 3.478 V, respectively, and the IR value of the first and last cycles is 0.0418  $\Omega$  and 0.0478  $\Omega$  value of the first and last cycles, respectively. In addition to that, its correlation coefficient is greater than 0.9 for all datasets as shown in Table I. Therefore,  $HI_R$  was found to be capable of reflecting the IR increase. Accordingly, we used it to estimate SOH based on resistance.

### B. SOH Estimation Framework

In existing approaches, the training process of SOH estimation is based on a single type of HI that either reflects capacity degradation or IR growth. However, capacity degradation and IR growth exhibit different behaviors, which might have different effects on the battery SOH. Therefore, it is only reasonable to consider both factors. Accordingly, we propose a battery health estimation method considering both capacity and IR. The overall proposed SOH estimation framework is illustrated in Fig. 1. This framework starts with the collection of the raw voltage and current data. Preprocessing

techniques were used before initializing the feature extraction process; these include: 1) data cleansing; and 2) normalization. Data cleansing is the process of removing outliers in the data to prevent underfitting and normalization is the process of scaling the data to values between 0 and 1. These techniques were performed offline and only in the training process. We computed data preprocessing during training. Then, precompute data preprocessing parameters are used during inference.

After data preprocessing, the features of the HIs were extracted. Then, the HIs were fed to the RNN to estimate the SOH. Specifically, a long short-term memory (LSTM) was employed to estimate  $SOH_c$  and  $SOH_r$ . Moreover, we specified the LSTM layer with 50 hidden units, followed by a fully connected layer of size 300 and a dropout probability of 0.5. The training epochs are set as 500 with mini-batches of size 50. We use the mean-square error as a loss function and the Adam optimizer as the optimization algorithm. These LSTM parameters are carefully tuned and determined by using cross-validation on the training data. Furthermore, in obtaining the SOH estimation model, data obtained from one battery cell (e.g., BEXEL cell #7: 492 measurement data) is used as a training set, and data obtained from another battery cell dataset (e.g., BEXEL cell #13: 438 measurement data) is used as a test set. This process was performed four times to have four test results.

In this letter,  $SOH_c$  is defined as the ratio of the initial battery capacity and its rated capacity [14]. Accordingly,  $SOH_c$  is 100% for a new battery (battery capacity is equal to the nominal capacity) and 0% when the capacity degrades to 80% of the nominal capacity.  $SOH_c$  is expressed as follows:

$$SOH_c = 1 - \frac{C_{int} - C_k}{0.2 \times C_{int}} \times 100\% \quad (2)$$

where  $C_{int}$  is the initial value of the battery capacity, and  $C_k$  is the capacity at the current cycle  $k$ . On the other hand,  $SOH_r$  is defined as the ratio of the increase in battery IR and the initial IR [14]. It is expressed as follows:

$$SOH_r = 1 - \frac{IR_{EOL} - IR_k}{IR_k - IR_{int}} \times 100\% \quad (3)$$

where  $IR_k$  is the IR at the current cycle  $k$ ,  $IR_{int}$  is the IR of a new battery, and  $IR_{EOL}$  is the IR value at the end of life where the presumed end of life threshold is 1.33 times of the nominal IR [10].

We estimated the SOH based on both  $SOH_c$  and  $SOH_r$ . Specifically, we treated the estimated SOH as a variable with two components: 1)  $SOH_c$ ; and 2)  $SOH_r$ . We hypothesized that both  $SOH_c$  and  $SOH_r$  have a significant effect on SOH. Therefore, neither of these could be neglected. To model the relationship between actual SOH,  $SOH_c$ , and  $SOH_r$ , we used the nonlinear least-square method in the MATLAB curve-fitting tool. The actual SOH is modeled using a second-degree polynomial surface function  $f(X, Y)$ , which is expressed as follows:

$$f(X, Y) = c_1 + c_2X + c_3Y - c_4X^2 - c_5Y^2 + c_6XY \quad (4)$$

where  $X$  is  $SOH_c$ ,  $Y$  is  $SOH_r$ , and  $c_n$ ,  $n = 1, \dots, 6$ , are the coefficients of the model.

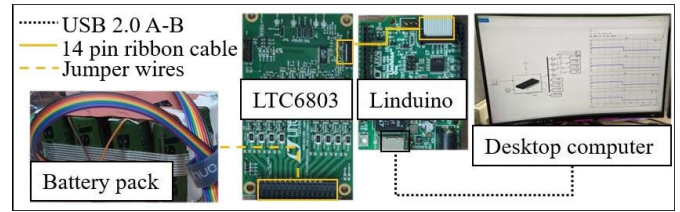


Fig.3. Configuration of the experimental platform.

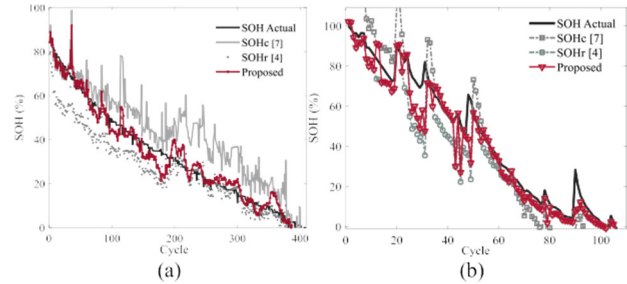


Fig.4. SOH estimation result: (a) BEXEL cell #7 and (b) NASACell #6.

### III. RESULTS AND DISCUSSION

#### A. Experimental Setup

The operation of the presented SOH estimation is evaluated using a proof-of-concept experimental setup. The experimental setup is shown in Fig. 3. It includes a BMS board with LTC6803 [15], Linduino Uno microcontroller board [15], a computer, and the BEXEL battery pack [12]. The BMS LTC6803 board is used to measure the first voltage value in the charging and discharging process as  $HI_{ch}$  and  $HI_{d}$ , respectively. Then, the Linduino Uno microcontroller transfers the  $HI_{ch}$  and  $HI_{d}$  to a computer. A computer with the Intel i5-6600 CPU 3.30 GHz is used to implement the real-time SOH estimation. Specifically, we create a function on Simulink that contains model weights and bias from trained LSTM. Then, we performed two scenarios: 1) the SOH estimation considering only capacity degradation or only IR growth; and 2) the SOH estimation considering both capacity degradation and IR growth.

#### B. Result of SOH Considering Capacity or IR Only

A single type of HI is represented as  $SOH_c$  and  $SOH_r$ . The estimated  $SOH_c$  and  $SOH_r$  were obtained based on capacity degradation and IR increase, respectively. As shown in Fig. 4(a),  $SOH_c$  can reflect the SOH from the 1st to the 200th charge cycle. After 200 cycles, the estimated  $SOH_c$  differed considerably from that of the actual SOH. On the other hand, the estimated  $SOH_r$  was considerably similar to that of the actual SOH. The gap between the estimated and the actual values of SOH indicates the different effects of capacity and IR on the actual SOH. This result shows that the SOH estimation method based on considering only either the capacity degradation or the IR growth is ineffective in reflecting the actual SOH.

#### C. Result of SOH Considering Capacity and IR

The proposed SOH estimation method considers both the estimated  $SOH_c$  and  $SOH_r$ . As depicted in Fig. 5(a), the estimated  $SOH_c$  and  $SOH_r$  exhibit a direct relationship with

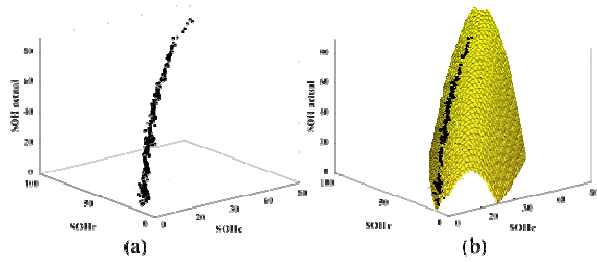


Fig. 5. SOH estimation result on BEXEL cell #7: (a) direct relationship between actual SOH,  $SOH_r$ ,  $SOH_c$ ; and (b) curve-fitting result.

TABLE II  
ERRORS IN RMSE AT DIFFERENT DATASETS

Datasets	[4]	[7]	Proposed	Proposed method improvement over [4] and [7] (%)	
				[4]	[7]
BEXEL cell #7	0.123	0.092	<b>0.041</b>	66.26	55.07
BEXEL cell #13	0.192	0.064	<b>0.033</b>	82.43	47.59
NASA cell #6	0.102	0.154	<b>0.036</b>	64.91	76.57
NASA cell #7	0.112	0.080	<b>0.028</b>	74.30	64.04

TABLE III  
COMPARISON OF TRAINING AND INFERENCE TIME

	[4]	[7]	Proposed
Avg. training time (s)	31	32	<b>46</b>
Avg. inference time (ms)	<b>39.5</b>	42.7	<b>30.6</b>

the actual SOH. The result of the best-fit curve is plotted in Fig. 5(b). This best-fit SOH model was approximated as a polynomial model, which is expressed as (4). The results in Fig. 4(a) and (b) reveal that SOH estimation is more accurate when both capacity degradation and IR growth are considered. Table II lists the estimation error obtained using our proposed method, [4], and [7]. In estimating the SOH, [4] considers only IR growth while [7] considers only capacity degradation. The estimation error is defined as the root-mean-square error (RMSE) between the actual SOH and the estimated SOH. Moreover, we specify the ranges of actual and predicted SOH is from 0 to 1. Hence, RMSE of 0.041 and 0.092 of the SOH estimations represents 4.1% and 9.2% estimation errors, respectively. Aside from the RMSE, Table II also lists the improvement in the accuracy of SOH estimation using the proposed method over [4] and [7]. Table II shows that the accuracy of SOH estimation using the proposed method has improved by up to 82.43% and 76.57% with BEXEL and NASA datasets, respectively. It reveals that the proposed model achieves substantially better performance than the other models based on single-type HIs.

We also present the comparison of training and inference time which are shown in Table III. Simulink execution time block which subtracting the timestamps for input and output signals is used to obtain inference time. In training, the extraction of HIs is not considered. While during inference, the extraction of HIs must be considered for real-time SOH estimation. Although the proposed method has the longest training time, this is not the addition of the training time for the benchmarking method. This is because we train the proposed

multiple simulations of a model in parallel. On the other hand, the inference time of the proposed method was reduced by an average of 29.20% even though more parameters are considered since the HIs are measurable. Moreover, the result reveals that the proposed method not only improved estimation accuracy but also reduced the computational complexity in real-time SOH estimation.

#### IV. CONCLUSION

In light of the clear correlation between the SOH predicted using capacity degradation and IR expansion, this letter suggests a real-time SOH estimation approach for embedded applications

1) Reducing the computational complexity in real-time SOH estimation while taking into account the battery health

#### REFERENCES

- [1] M. V. Reddy, A. Mauger, C. M. Julien, A. Paoella, and K. Zaghib, "Brief history of early lithium-battery development," *Materials*, vol. 13, no. 8, p. 1884, 2020.
- [2] W. Liu and Y. Xu, "Data-driven online health estimation of Li-ion batteries using a novel energy-based health indicator," *IEEE Trans. Energy Convers.*, vol. 35, no. 3, pp. 1715–1718, Sep. 2020.
- [3] F. Liu, X. Liu, W. Su, H. Lin, H. Chen, and M. He, "An online state of health estimation method based on battery management system monitoring data," *Int. J. Energy Res.*, vol. 44, no. 8, pp. 6338–6349, 2020.
- [4] A. Eddahech, O. Briat, N. Bertrand, J.-Y. Deléage, and J.-M. Vinassa, "Behavior and state-of-health monitoring of Li-ion batteries using impedance spectroscopy and recurrent neural networks," *Int. J. Electr. Power Energy Syst.*, vol. 42, no. 1, pp. 487–494, 2012.
- [5] M. K. S. Verma *et al.*, "On-board state estimation in electrical vehicles: Achieving accuracy and computational efficiency through an electrochemical model," *IEEE Trans. Veh. Technol.*, vol. 69, no. 3, pp. 2563–2575, Mar. 2020.
- [6] E. Chemali, "Intelligent state-of-charge and state-of-health estimation framework for Li-ion batteries in electrified vehicles using deep learning techniques," Ph.D. dissertation, Dept. Electr. Comput. Eng., McMaster Univ., Hamilton, ON, Canada, 2018.
- [7] J. Qu, F. Liu, Y. Ma, and J. Fan, "A neural-network-based method for RUL prediction and SOH monitoring of lithium-ion battery," *IEEE Access*, vol. 7, pp. 87178–87191, 2019.
- [8] S. Shen, M. Sadoughi, X. Chen, M. Hong, and C. Hu, "A deep learning method for online capacity estimation of lithium-ion batteries," *J. Energy Storage*, vol. 25, Oct. 2019, Art. no. 100817.
- [9] H. Chaoui and C. C. Ibe-Ekeocha, "State of charge and state of health estimation for lithium batteries using recurrent neural networks," *IEEE Trans. Veh. Technol.*, vol. 66, no. 10, pp. 8773–8783, Oct. 2017.
- [10] A. Guha and A. Patra, "State of health estimation of lithium-ion batteries using capacity fade and internal resistance growth models," *IEEE Trans. Transport. Electrification*, vol. 4, no. 1, pp. 135–146, Mar. 2018.
- [11] B. Saha and K. Goebel, *Battery Data Set: NASA AMES Prognostics Data Repository*. NASA AMES Res. Center, Mountain View, CA, USA, 2007. [Online]. Available: <http://ti.arc.nasa.gov/project/prognostic-data-repository>
- [12] Bexel. *BEXEL Battery Company Profile*. Accessed: Jan. 6, 2021. [Online]. Available: <http://www.bexel.co.kr/>
- [13] J. L. Rodgers and W. A. Nicewander, "Thirteen ways to look at the correlation coefficient," *Amer. Stat.*, vol. 42, no. 1, pp. 59–66, 2012.

- [14] L.Chen,Z.Lü,W.Lin,J.Li,andH.Pan,“Anewstate-of-healthestimation method for lithium-ion batteries through the intrinsic relationshipbetweenohmicinternalresistanceandcapacity,”*Measurement*,vol.116, pp.586–595,Feb.2018.
- [15] *Overview of LTC6803 and Linduino (Documentation, and Ordering)*,Accessed: Mar. 2, 2020. [Online]. Available: <https://www.analog.com/en/products/ltc6803-1>